 CMC, vol.31, no.3, pp.229-251, 2012

Evaluation of Fracture Parameters by Double-G, Double-K Models and Crack Extension Resistance for High Strength and Ultra High Strength Concrete Beams

A. Ramachandra Murthy[1], Nagesh R. Iyer[1] and B.K. Raghu Prasad[2]

Abstract: This paper presents the advanced analytical methodologies such as Double- G and Double – K models for fracture analysis of concrete specimens made up of high strength concrete (HSC, HSC1) and ultra high strength concrete. Brief details about characterization and experimentation of HSC, HSC1 and UHSC have been provided. Double-G model is based on energy concept and couples the Griffith's brittle fracture theory with the bridging softening property of concrete. The double-K fracture model is based on stress intensity factor approach. Various fracture parameters such as cohesive fracture toughness (K_{Ic}^{c}), unstable fracture toughness (K_{Ic}^{un}) and initiation fracture toughness (K_{Ic}^{ini}) have been evaluated based on linear elastic fracture mechanics and nonlinear fracture mechanics principles. Double-G and double-K method uses the secant compliance at the peak point of measured P-CMOD curves for determining the effective crack length. Bi-linear tension softening model has been employed to account for cohesive stresses ahead of the crack tip. From the studies, it is observed that the fracture parameters obtained by using double – G and double – K models are in good agreement with each other. Crack extension resistance has been estimated by using the fracture parameters obtained through double – K model. It is observed that the values of the crack extension resistance at the critical unstable point are almost equal to the values of the unstable fracture toughness K_{Ic}^{un} of the materials. The computed fracture parameters will be useful for crack growth study, remaining life and residual strength evaluation of concrete structural components.

1 Introduction

Concrete has been one of the most commonly used construction materials in the world. One of the major problems civil engineers face today is concerned with

[1] CSIR-Structural Engineering Research Centre, Taramani, Chennai, India, 600113, [murthyarc, nriyer] @serc.res.in

[2] Civil Engineering Dept., Indian Institute of Science, Bangalore, bkr@civil.iisc.ernet.in

preservation, maintenance and retrofitting of structures. The historical development of concrete material may be marked and divided into several stages. The first is the traditional normal strength concrete and followed by high strength concrete, high performance concrete and reactive powder concrete/ultra high strength concrete. Since UHSC is a relatively new material, the fracture behaviour of this material is not well understood (Richard and Cheyrezy 1994, 1995, Mingzhe et al. 2010, Goltermann et al. 1997).

Over the last three decades, one of the main developments in the application of the fracture mechanics to concrete is the identification of cohesive forces across the fracture process zone in front of the apparently stress-free crack, based on extensive experimental investigations using various measurement methods by many researchers. As a consequence, the fictitious crack model was proposed by Hillerborg et al. (1976) and the crack band model by Bazant and Oh (1983). Both of them have been widely applied to the numerical analysis of concrete structures. To determine the softening traction-separation law for concrete, many expressions were proposed based on direct tensile tests (Rama Chandra Murthy et al. 2008).

Finite element or boundary element methods can be employed to analyze cohesive crack model and crack band model, which take into account of fracture process zone by means of constitutive relations showing strain softening and strain localization during the crack propagation. Crack band model and cohesive crack model are equivalent to each other when the path of the crack (or crack band) is known *a priori*. The band thickness in case of the crack band model is reduced to zero. Cohesive crack model is more popular because of its simplicity and ability to represent the real physical process and describe the nonlinear fracture behavior of the material. The modified linear elastic fracture models are based on stress intensity factor (SIF) concept except the double-G fracture model, which is based on the energy release rate approach. Apart from the external load, crack length and specimen geometry, the fracture energy release rate approach also depends on the deformation characteristic (Young's modulus) of the material. Hence, ductility property is also associated with energy release rate approach unlike that of SIF based models.

Many researchers proposed many fracture models, among which the typical models are, two parameter fracture model (TPFM) (Jenq and Shah 1985), size effect model (SEM) (Bazant et al. 1987), effective crack model (ECM) (Karihaloo and Nallathambi 1990, Swartz and Refai 1987) and double-K fracture model (DKFM) (Xu and Reinhardt 1999 Xu and Reinhardt 2000). For the first two, RILEM Technical Committee 89-FMT made the detailed discussions and drafted the experimental procedures for the determination of the fracture toughness of concrete (Jenq and Carpinteri 1991, Bazant and Kazemi 1989 RILEM Technical Committee 1990). For comparison, the effective crack model was discussed in RILEM's technology

report as well (Jenq and Carpinteri 1991). In these three models, only critical unstable state during the entire crack propagation is highlighted. However, various experimental investigations using different approaches have confirmed that the crack propagation in concrete experiences three distinguished stages: crack initiation, stable crack propagation and unstable fracture (Xu and Reinhardt 1999, Horii and Ichinomiya 1991)

Due to lack of knowledge of crack initiation resistance, it is not clearly known whether the stable crack propagation will occur. This is rather important for concrete structures, which are heterogeneous and quasi-brittle. As a result, it is necessary for such structures to introduce another fracture parameter as the threshold of onset of stable crack propagation to predict whether stable crack propagation stage will occur. Because of this, Xu and Reinhardt (1999) developed double-K fracture model, in which besides employing the unstable fracture toughness K_{Ic}^{un} as a fracture controlling parameter, another notation K_{Ic}^{ini} that was defined as the initiation fracture toughness was introduced. In addition, this model considers that the initiation and unstable fracture toughness are inter-related, and that the difference between them is assumed to the contribution of aggregate bridging stress distributed across crack face. Based on this assumption, the mathematical formulae to determine the two fracture parameters were proposed, and substantive numerical simulations and experimental work to examine the effect of size, geometry and strength on them were systematically carried out (Xu and Reinhardt 1999 Xu and Reinhardt 2000)

The double-K fracture model is based on SIF. In order to determine the value of cohesive toughness in double-K fracture model, a specialized numerical treatment is needed because of the singularity at the crack tip. A simplified approach (Xu and Reinhardt 2000) was later proposed using two empirical formulae to obtain the double-K fracture parameters for three-point bending configuration, which avoided the need of specialized numerical technique for determining the values of cohesive toughness and trial and error approach for computing the value of effective crack length during crack propagation. A little later, an energy-based model was developed similar to double-K fracture model by Zhao and Xu (2002). It is called double-G model. Similar to the double-K fracture model, again, mortar matrix was assumed to behave in the same manner as the brittle materials. Moreover, the nonlinearity of fracture behaviour exhibited in concrete is supposed to be caused fully by the bridging cohesive action of aggregates. Therefore, two governing parameters, i.e., the initiation fracture energy release G_{Ic}^{ini} standing for the Griffith fracture surface energy of mortar matrix, and the unstable fracture energy release G_{Ic}^{un} representing the energy required to overcome the common resistance of mortar matrix and aggregates at the critical unstable state, were introduced in this model to predict

at which stage crack propagation is occurring. In addition, energy consumption due to aggregate cohesive resistance is linked to the proposed two fracture parameters (Xu and Zhang 2008)

In the present work, fracture parameters have been evaluated for high strength concrete and ultra high strength concrete by using double –G and double –K concepts. Crack extension resistance has been estimated by using the fracture parameters obtained through double -K model.

2 Experimental Investigation

Three different mixes designated as high strength concrete (HSC, HSC1), and Ultra High Strength Concrete (UHSC) are characterized and their mix proportions have been derived using appropriate method and several trials. For HSC, the ingredient materials are Portland cement, coarse aggregate, fine aggregate and water, whereas for HSC1, the materials are Portland cement, silica fume, quartz sand, high range water reducer, water and steel fibers. Further, for UHSC, the materials are Portland cement, silica fume, quartz sand, quartz powder, high range water reducer, water and steel fibers. The main difference between HSC1 and UHSC is the absence of quartz powder in the case of HSC1 mix. Bureau of Indian Standard code has been used for HSC mix design whereas for HSC1 and UHSC mixes have been designed based on the limited literature available and several trials.

Several trials had to be tried before a final mix design. The final mix proportions and ratio obtained are given in Tables 1 and 2.

Table 1: Mix Proportions for HSC, HSC1 and UHSC

Property	HSC	HSC1	UHSC
Water/cement ratio	0.45	0.33	0.23
Cement, kg/m^3	452.44	811.7	838.93
Silica fume, kg/m^3	-	202.9	209.73
Quartz sand, kg/m^3	-	1217.5	922.82
Quartz powder, kg/m^3	-	-	335.57
Fine aggregate, kg/m^3	565.55	-	-
Coarse aggregate, kg/m^3	1127.01	-	-
Water, kg/m^3	203.6	267.9	192.95
Steel Fiber, kg/m^3		157.20	158.50
Superplasticizer, (% weight of cement content in mix)	-	2.5%	3.5 %

Table 2: Mix ratio of HSC, HSC1 and UHSC

Mix	Cement	Fine aggregate	Coarse aggregate	Silica fume	Quartz sand	Quartz powder	Steel fiber	w/c	SP %
HSC	1	1.25	2.48	-	-	-	-	0.45	-
HSC1	1	-	-	0.25	1.5	-	2%	0.33	2.5
UHSC	1	-	-	0.25	1.1	0.4	2%	0.23	3.5

2.1 Specimen Preparation

Preparation, demoulding and curing of HSC specimens is as usual whereas the procedure for specimen preparation for HSC1 and UHSC is outlined below.

- A Hobart mixer machine (15 kg capacity) or Eirich type mixer (150 liter capacity) is used to mix the concrete mixtures.
- Well mixed dry binder powder is then slowly poured in to the bowl while the mixer is rotating at a slow speed.
- The speed of the mixer is increased and the mixing process is continued for about two to three minutes.
- Water is then added.
- Additional mixing is performed at this speed until a uniform mixture is achieved.
- Fibers are added after mixing all the ingredients such as cement, quartz sand, quartz powder and silica fume with water and superplasticizer.
- Fresh mixture is poured in to the moulds using a steel scoop.
- Compaction is done by placing the filled moulds on a laboratory table vibrator for about 2 minutes.
- The specimens are demoulded after a lapse of 24 hours.
- Immediately after demoulding, the specimens are fully immersed in potable water at room temperature for 2 days. After 2 days of normal water curing, the specimens are placed in a autoclave and maintained at 90˚C for 2 days. Further, the specimens are placed in oven and maintained at 200˚C for 1 day followed by autoclave curing.

Cubes and cylinders have been cast based on the above procedure.

2.2 Mechanical Properties

Mechanical properties such as compressive strength, spilt tensile strength of HSC, HSC1 and UHSC mix at 28 days are shown in Table 3. From Table 3, it can be observed that the split tensile strength for the case of HSC is 4.0 MPa. It is about 7% of compressive strength. In the case of HSC1, the split tensile strength is about 18% of compressive strength. The increase in strength is large compared to HSC. The increase in strength may be due to various sizes of ingredients and steel fibres. Further, it can be observed from Table 3 that UHSC has high compressive strength and tensile strength. The high strengths can be attributed to the contribution at different scales viz., at the meso scale due to the fibers and at the micro scale due to the close packing of grains which is on account of good grading of the particles.

Table 3: Mechnanical properties of HSC, HSC1 and UHSC

Mix ID	Compressive Strength (MPa)	Split tensile Strength (MPa)	Modulus of elasticity (MPa)
HSC	57.14	3.96	35,780
HSC1	87.71	15.38	37,890
UHSC	122.52	20.65	42,987

Different beams, namely, small, medium and large size with various notch depths have been cast to study the fracture behaviour. The experimental setup consists of a MTS 2500 kN capacity servo hydraulic UTM with online data acquisition system. The loading frame is a material testing system (MTS) with data acquisition and all the specimens have been tested under displacement control at a rate of 0.02 mm/min. The midspan downward displacement is measured using linear variable displacement transducer (LVDT), placed at center of the specimen under bottom of the beam. A clip gauge is used to measure the crack mouth opening displacement (CMOD). The data acquisition records load, CMOD, mid-span displacement and time. Appropriate load cells have been used for load application during testing. Compliance curves have been generated to estimate the crack initiation load and critical crack length. Typical load-CMOD diagrams under quasi-static cyclic loading of small, medium and large size beams of HSC and UHSC are presented in Figures. 1 to 6.

3 Double-G Fracture Model

This model is based on energy concept and couples the Griffith's brittle fracture theory with the bridging softening property of concrete. In this model, two fracture parameters, i.e the initiation fracture energy release G_{Ic}^{ini} and unstable fracture

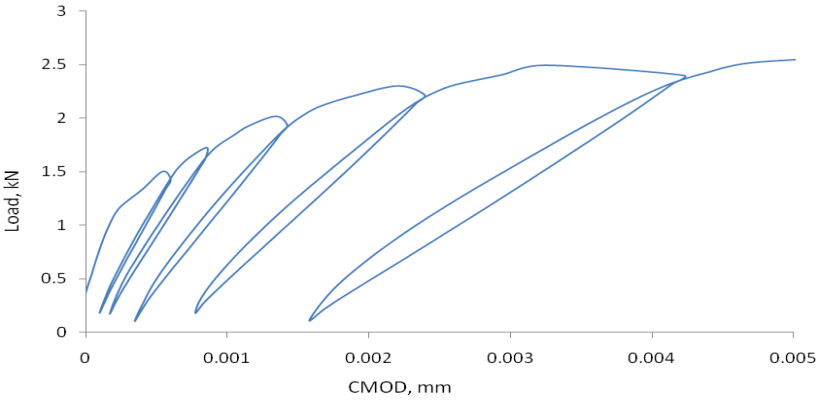

Figure 1: Load vs CMOD for HSC – Small size beam (notch depth = 5 mm)

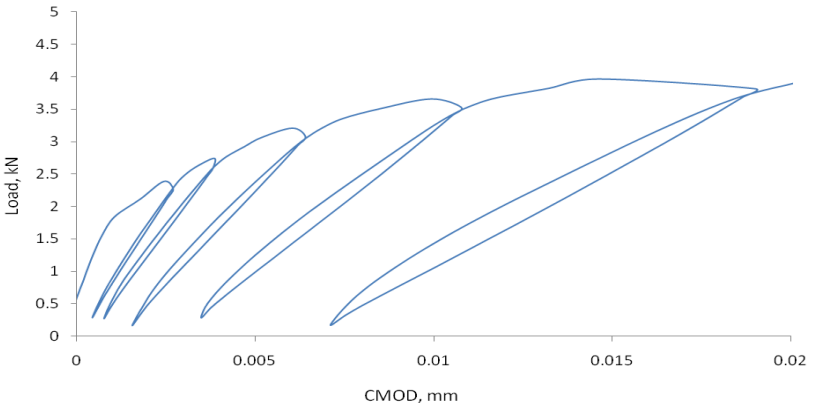

Figure 2: Load vs CMOD for HSC – Medium size beam (notch depth = 10 mm)

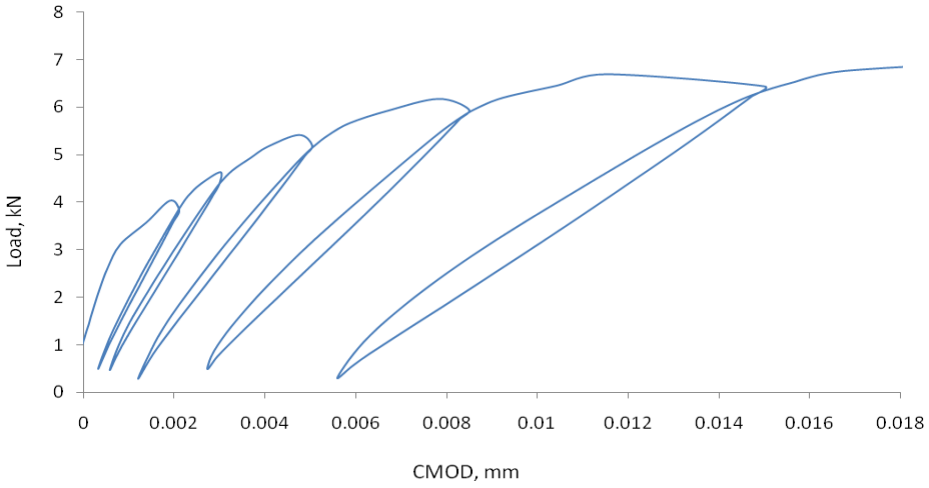

Figure 3: Load vs CMOD for HSC – large size beam (notch depth = 20 mm)

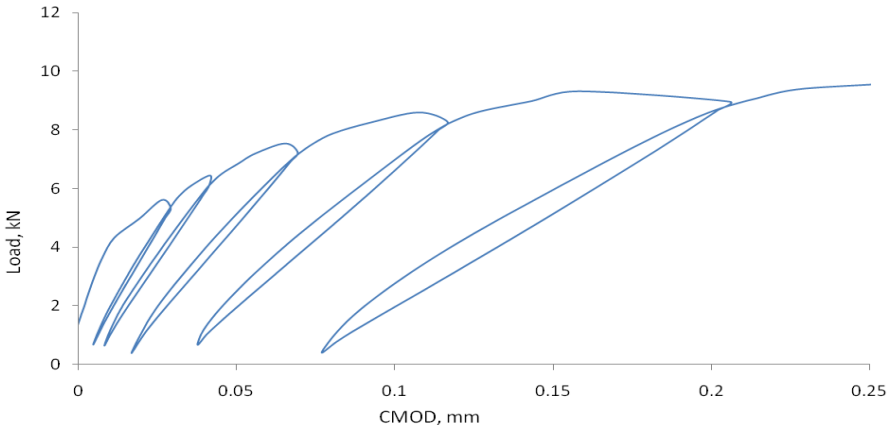

Figure 4: Load vs CMOD for UHSC – Small size beam (notch depth = 5mm)

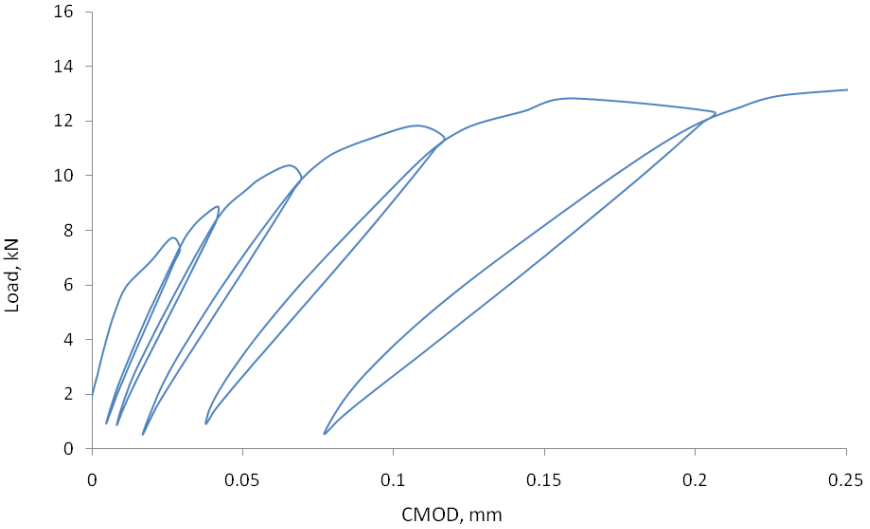

Figure 5: Load vs CMOD for UHSC – Medium size beam (notch depth = 8mm)

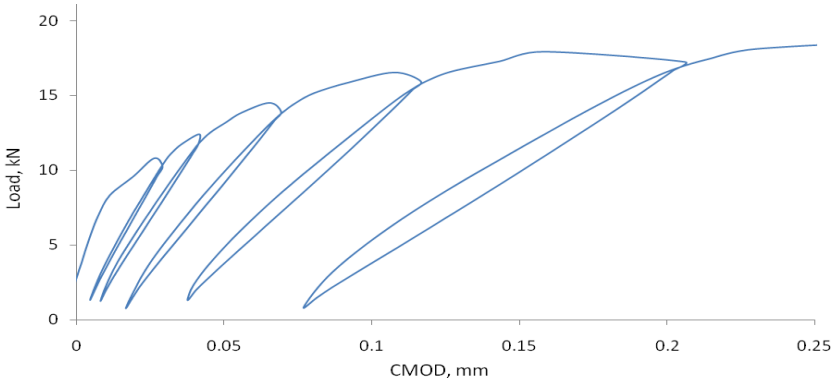

Figure 6: Load Vs CMOD for UHSC – Large size beam (notch depth = 13mm)

energy release G_{Ic}^{un}, are termed to distinguish the different crack propagation stages undergoing during the whole fracture process in concrete. The value of G_{Ic}^{ini} is defined as the Griffith fracture surface energy of concrete mix in which the matrix remains still in elastic state under the initial cracking load $P_{ini}$and the initial crack length a_0.Once the load value P on the structure is increased beyond the value of P_{ini}, a new crack surface (macro-cracking) is formed and the cohesive stress along the new crack surface starts acting. The cohesive stress provides additional resistance to the stable crack propagation in terms of cohesive breaking energy G_{Ic}until the critical condition is achieved. At the onset of unstable crack propagation or critical condition, the total energy release is G_{Ic}^{un} from which K_{Ic}^{un} is obtained. The difference between the two parameters, G_{Ic}^{un} & G_{Ic}^{ini} written as G_{Ic}^{C} is assumed to come from the contribution by aggregate bridging interlock, which results in the presence of fracture process zone.

The major steps of the model are given below.

(i) Energy release rate can be calculated by (Tada 1985)

$$G = \frac{P^2 dc}{2Bd\alpha} \tag{1}$$

where, $\frac{dc}{d\alpha}$ = change of compliance with crack propagation

When compliance for any given geometry is known, equation (6.1) can be used to obtain the energy release rate.

For a three point bending beam as shown in Figure 7, the compliance expression can be found in Tada's crack analysis handbook (Tada 1985).

$$C = \frac{\delta}{P} = \frac{3S^2}{2BD^2E} V(\alpha) \tag{2}$$

where, $V(\alpha) = \left(\frac{\alpha}{1-\alpha}\right)^2 \left(5.58 - 19.57\alpha + 36.82\alpha^2 - 34.94\alpha^3 + 12.77\alpha^4\right)$ and $\alpha = (a + H_o)/(D + H_o)$

a : effective crack length, H_o: thickness of knife edge for clip extension gauge holder, S, D are span and depth of the specimen respectively.

On differentiating equation (2) w.r.t the effective crack depth ratio, the value of $dc/d\alpha$ for three point bending beam can be obtained, as

$$\frac{dc}{d\alpha} = \frac{d}{d\alpha}\left(\frac{\delta}{P}\right) = \frac{3S^2}{2BD^3E} V'(\alpha) \tag{3}$$

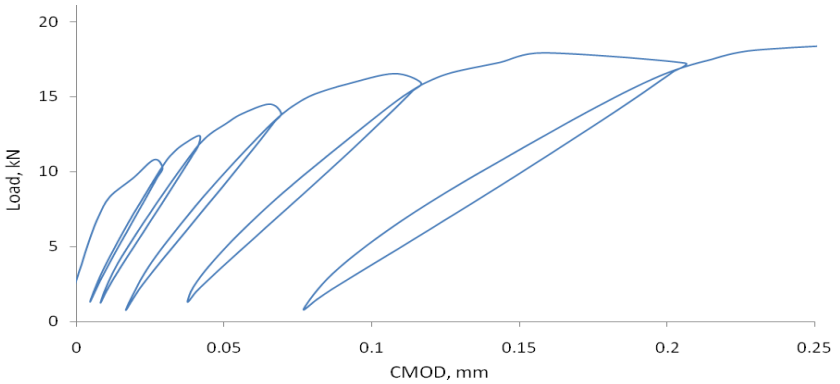

Figure 7: Three-point bending beam

where

$$v'(\alpha) = \frac{2\alpha}{(1-\alpha)^3}(5.58 - 19.57\alpha + 36.82\alpha^2 - 34.94\alpha^3 + 12.77\alpha^4) + \left(\frac{\alpha}{1-\alpha}\right)^2(-19.57 + 73.64\alpha - 104.82\alpha^2 + 51.08\alpha^3) \tag{4}$$

(ii)The initiation fracture energy release G_{Ic}^{ini} can be computed by using P_{ini} at point A (refer Figure 8) and initial crack length a_o

$$G_{Ic}^{ini} = \frac{3P_{ini}^2 S^2}{4B^2D^3E}V'(\alpha_o) \tag{5}$$

(iii) To determine, the unstable fracture energy release,G_{IC}^{un}, another fracture parameter in double-G fracture model viz., the critical effective crack length must be known. The value of the critical effective crack length a_c is obtained by assuming linear asymptotic superposition (Xu and Reinhardt 2000). The simple formula to evaluate the propagating crack length is rewritten as follows:

$$\begin{aligned} a_c &= \frac{2}{\pi}(D+H_0)\ arc\tan\sqrt{\frac{BECMOD}{32.6P} - 0.1135} - H_0 \\ &= \frac{2}{\pi}(D+H_0)\ arc\tan\sqrt{\frac{BEc_s}{32.6} - 0.1135} - H_0 \end{aligned} \tag{6}$$

where, a_c is the propagating crack length; C_s is the secant compliance, i.e.,$C_s = CMOD/P$.

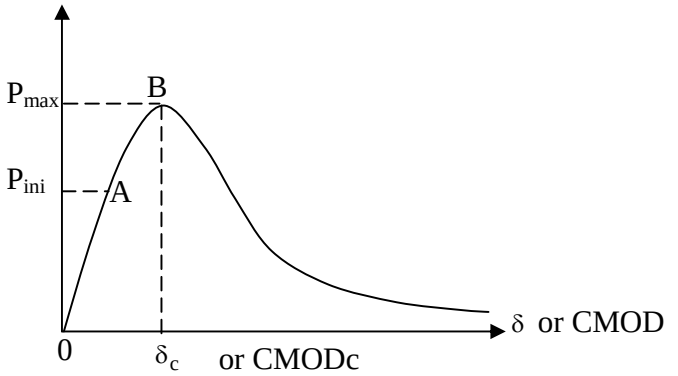

Figure 8: Typical load-loading line displacement curve ($P-\delta$ *or* $P-CMODc$)

By replacing P_{ini} and a_o with the maximum load $P_{\max}$ corresponding to point B (Figure 8) and the critical effective crack length a_c given in equation (6), the unstable fracture energy release G_{Ic}^{un} can be determined using the following equation (7).

$$G_{Ic}^{un} = \frac{3P_{\max}^2 S^2}{4B^2 D^3 E} v'(\alpha_c) \tag{7}$$

To summarise the entire fracture process in concrete, the total energy dissipation for extending unit length crack at any crack propagation can be divided into two parts: the contribution by mortar matrix and that by aggregate bridging cohesive property.

The critical cohesive breaking energy is G_{Ic}^{c} can be computed by using the following expression

$$\text{(iv)} \quad G_{Ic}^{c} = G_{Ic}^{un} - G_{Ic}^{ini} \tag{8}$$

G_{Ic}^{c} is the average value of energy dissipation in FPZ at maximum load.

(v) Computation of SIF (K)

In the linear stage, fracture behaviour can be considered to be elastic, where formula in LEFM such as $K = \sqrt{EG}$ holds true. In the non-linear stage, LEFM is not suitable to describe the fracture behaviour of concrete material. In this stage, $K = \sqrt{EG}$ can not be applied. But, fracture process zone, which is responsible for non-linear characteristics of concrete fracture may be changed into a series of linear parts by an equivalent elastic approach. By this approach, LEFM can again be used to evaluate fracture parameters of concrete. Hence, the effective double-K fracture parameters, written as, K_{Ic}^{ini} and K_{Ic}^{un} are calculated by $K = \sqrt{EG}$.

4 Double-K Facture Model

In the case of double-K model, cohesive fracture toughness K_{Ic}^{C} and unstable fracture toughness K_{Ic}^{un} are evaluated and the difference between the K_{Ic}^{un} and K_{Ic}^{C} is termed as initiation toughness K_{Ic}^{ini}.

$$K_{Ic}^{ini} = K_{Ic}^{un} - K_{Ic}^{C} \tag{9}$$

K_{Ic}^{C} is evaluated by knowing the bi-linear tension softening relationship, which is obtained from the inverse analysis and K_{Ic}^{un} is evaluated by using LEFM principles. The major steps for evaluation of K_{Ic}^{un} and K_{Ic}^{C} are given below:

(i) Evaluate K_{Ic}^{un}

$$K_{Ic}^{un} = \frac{3P_{\max}S}{2D^2B}\sqrt{a_c}F_1(V_c) \tag{10}$$

where, $V_c = a_c/D$

(ii) Evaluate K_{Ic}^{C}

SIF, K_{Ic}^{c} caused by a cohesive stress $\sigma(x)$ on the fictitious crack zone in the critical state for the considered three point notched bending beam is analysed by equivalent point force concept (Xu and Reinhardt 2000). For the distributed cohesive force and boundary condition shown in Figure 9, SIF K_{Ic}^{c} at the crack tip can be calculated by using the following expression

$$K_{Ic}^{C} = -\int_{a_0}^{a} \frac{2\sigma(x/a)}{\sqrt{\pi a}}\ F\left(\frac{x}{a}, \frac{a}{D}\right) dx (a \le a_c) \tag{11}$$

where, a_c is the crack length at a critical situation.

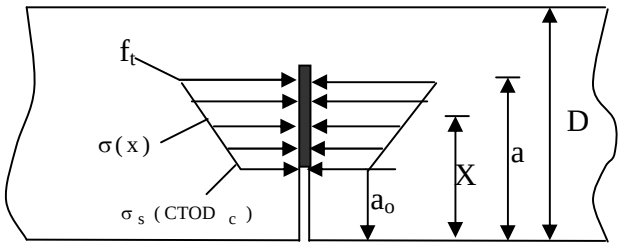

Figure 9: Cohesive force on the fictitious crack zone at the critical situation

As mentioned earlier, bi-linear tension softening relationship derived by using the inverse analysis has been used to account for the cohesive stresses acting ahead of the crack tip.

More details about the double-G and double-K models are available in Xu and Zhang (2008), Xu and Reinhardt (1999, 2000).

5 Crack Extension Resistance

The concept of R-curve was first introduced using the energy criterion by Irwin (1958) for fracture of metals. R-curve approach has been widely used for fracture of cementitious composites and ceramics in recent times (Jenq and Shah 1985, Hsueh and Becher 1988). Since then many attempts have been made to theoretically construct and experimentally measure the R-curve. The major difficulty in the study of R-curve behaviour is that it depends on both the specimen geometry and material parameters. Wecharatana and Shah (1982) have used the R-curve to model the stable crack growth in concrete. Cook and Fairbanks (1987) assumed that R-curve is a power function with two geometry dependent constants. Li and Liang (1992) proposed a stability theory for crack propagation based on the fictitious crack approach. Bazant et al. (1986) proposed the R-curve for any given geometry, which can be determined on the basis of the size effect law.

Recently, Xu and Reinhardt (1998, 1999) and Reinhardt and Xu (1999) introduced K_R-curve method for complete fracture process description of concrete. Their approach differs from the conventional method originally proposed by Irwin (1958) and Kraft et al. (1961) in early 1960s. The distribution of cohesive stress along the fictitious fracture zone at different stages of loading conditions are taken into account in order to evaluate the K_R-curve for three-point bending test of concrete beam (Xu and Reinhardt (1998, 1999).

The graphical representation of K_R curve is shown in Figure 10.

In general, when

$K_I < K_{Ic}^{ini}$ - no crack propagation appears, $K_I = K_{Ic}^{ini}$ - crack starts to propagate steadily,

$K_{Ic}^{ini} < K_I < K_{Ic}^{un}$ – crack propagates steadily, $K_I = K_{Ic}^{un}$ - critical unstable crack propagation begins, $K_I > K_{Ic}^{un}$ - crack propagates unsteadily.

For a cracked solid structure, one can calculate a curve of the SIF created by an acting extra load at the tip of a propagating crack and can measure the crack extension resistance curve of the material, which is composed of the inherent toughness, which represents the elastic characteristics of the material, and the cohesive toughness, which increases with the increase of the amount of crack extension. The use of the two curves is to judge instability of a propagating crack in a solid structure. According to the above-mentioned $K_R(\Delta a)$ includes two parts, which are expressed

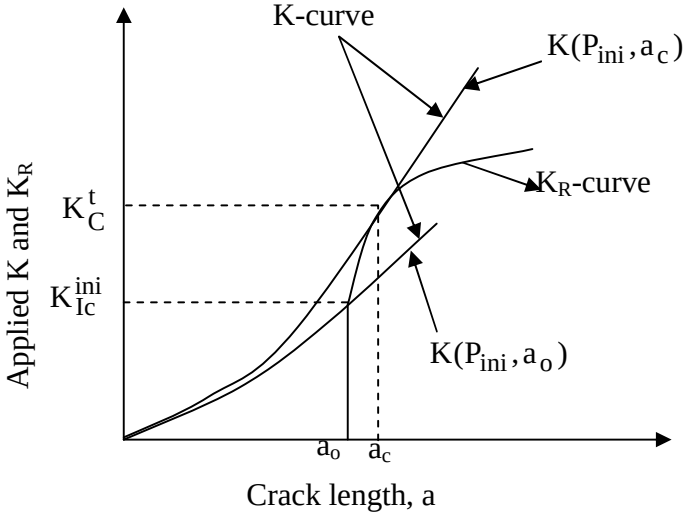

Figure 10: Graphical representation of the K_R-curve

as follows:

$$K_R(\Delta a) = K_{Ic}^{ini} + K_{Ic}^{c}(\Delta a) \tag{12}$$

where,

$$K_{Ic}^{c}(\Delta a) = F\left(f_t, f(\sigma), \Delta a\right) \tag{13}$$

The function $F\left(f_t, f(\sigma), \Delta a\right)$ is mainly dependent on the tensile strength f_t of the tested material and the length of the fictitious crack zone and slightly affected by the distribution shape of the cohesive force along the fictitious crack zone (Xu and Reinhardt 1998).

K_{Ic}^{ini} is evaluated based on LEFM principles and $K_{Ic}^{C}$is evaluated using double-K model.

6 Numerical Studies

Numerical studies have been conducted to validate the methodologies described in the previous sections to determine the various fracture parameters. Experimental results and the bi-linear tension softening relationship obtained from the inverse analysis are used for evaluation of fracture parameters. Fracture parameters have been evaluated based on double – G and double – K models. Crack extension resistance is estimated by using the fracture parameters obtained through double –

K model. Table 1 shows the input values required for fracture analysis by using double-G, double-K and crack extension resistance concepts.

In case of double – G model, K_{Ic}^{ini} and K_{Ic}^{un} are obtained by using LEFM principles. K_{Ic}^{c} is evaluated as the difference of K_{Ic}^{un} and K_{Ic}^{ini}. In the case of double – K model, K_{Ic}^{ini} is obtained as the difference of K_{Ic}^{un} and K_{Ic}^{c}. K_{Ic}^{un} is computed by using LEFM principles and K_{Ic}^{c} is computed by accounting the cohesive stresses ahead of crack tip. For the evaluation of K_{Ic}^{c}, bi-linear tension softening model obtained from inverse analysis is used. From Tables 1 to 3, it can be observed that the computed fracture parameters K_{Ic}^{c}, K_{Ic}^{un} and K_{Ic}^{ini} obtained from double – G and double – K models are in very good agreement with each other.

Crack extension resistance parameter $K_R(\Delta a_c)$ is obtained as the sum of initiation fracture toughness K_{Ic}^{ini} and cohesive fracture toughnessK_{Ic}^{C}. The initiation fracture toughness K_{Ic}^{ini} and K_{Ic}^{un} is evaluated by using LEFM principles. The relative ratios of $K_R(\Delta a_c)$ to K_{Ic}^{un} are given in Tables 2 to 4.

In general, from crack extension resistance, it can be noted that

$K(P,a) < K_R(\Delta a))$ – crack propagates steadily

$K(P,a) = K_R(\Delta a))$ – critical unstable crack propagation occurs

$K(P,a) \geq K_R(\Delta a))$ – crack propagates unsteadily

It can be observed from Table that K_{Ic}^{ini}value evaluated using double-K model and using LEFM principles are not the same. The reason is that in the case of double-K model, K_{Ic}^{ini} is obtained as the difference of K_{Ic}^{un} and K_{Ic}^{C}. The value of K_{Ic}^{C} is evaluated by approximating the softening behaviour as bi-linear. Hence, for the evaluation of crack extension resistance, K_{Ic}^{ini} evaluated by using LEFM principles is used and is named as K_{Ic}^{ini}(r). From Tables 2 to 4, it can be observed that the values of the crack extension resistance at the critical unstable point $K_R(\Delta a_c)$are almost equal to the values of the unstable fracture toughness K_{Ic}^{un} of the materials.

7 Summary

Advanced analytical methodologies such as double- G and double – K models for fracture analysis of concrete specimens have been described. Double-G and double-K method uses the secant compliance at the peak point of measured P-CMOD curves for determining the effective crack length. Various fracture parameters such as K_{Ic}^{c}, K_{Ic}^{un} and K_{Ic}^{ini} are evaluated based on LEFM and NLFM principles. Bi-linear tension softening model has been employed to account for cohesive stresses ahead of the crack tip. It is observed that the fracture parameters obtained by using double – G and double – K models are in good agreement with each other. Crack extension resistance has been estimated by using the fracture parameters ob-

Table 4: Input values for fracture analysis

Beam dimensions, mm	Notch depth, mm	P_{ini} N	P_u N	a_c mm	$CMOD_c$ mm
HSC – 250*50*50	5	2099	2624	28.12	0.0275
	10	1584	1981	26.3	0.0208
	15	1060	1060	24.87	0.0201
HSC-500*50*100	10	3627	4534	54.3	0.0155
	20	3096	3870	52.3	0.0155
	30	2060	2575	48.2	0.0118
HSC-1000*50*200	20	5819	7274	110.6	0.0280
	40	5120	6278	104.6	0.0392
	60	3648	4560	98.4	0.0625
HSC1- 250*50*50	5	2101	4203	33.43	0.4543
	10	1685	3121	32.45	0.6321
	15	1535	2791	31.89	0.5123
	20	1060	1983	30.98	0.5643
HSC1-500*50*100	10	4590	8346	55.67	0.8654
	20	2857	5102	54.76	0.7612
	30	2129	3802	53.65	0.6618
	40	1677	2994	51.98	0.6123
UHSC-250*50*50	5	5878	10136	33.5	0.8317
	10	4510	7812	32.65	0.5383
	15	3552	6128	31.76	0.6183
	20	2357	4065	30.75	0.6432
UHSC-400*50*80	8	8878	14798	56.25	0.3421
	16	6293	10851	55.35	0.4311
	24	4414	7612	53.12	0.5213
	32	3227	5564	52.14	0.5432
UHSC-650*50*130	13	11302	19487	89.3	1.3372
	26	7850	13367	87.3	0.8654
	39	5879	10121	86.54	0.7654
	52	4326	7460	83.45	0.6543

Table 5: Fracture parameters of HSC

Beam dimensions (mm)	Notch depth (mm)	Fracture parameters (MPa$\sqrt{\text{m}}$)						Crack extension resistance using Double – K model	
		Double-G model			Double-K model			$K_R(\Delta a_c) = K_{Ic}^{ini}(r) + K_{Ic}^{C}$	Ratio, $\frac{K_R(\Delta a_c)}{K_{Ic}^{un}}$
		K_{Ic}^{ini}	K_{Ic}^{un}	K_{Ic}^{C}	K_{Ic}^{ini}	K_{Ic}^{un}	K_{Ic}^{C}		
250*50*50	5	0.81	1.34	0.53	0.75	1.35	0.60	1.34	0.99
	10	0.77	1.16	0.39	0.71	1.11	0.40	1.11	1.00
	15	0.65	0.95	0.30	0.61	0.91	0.30	0.92	1.01
500*50*100	10	0.89	1.57	0.69	0.72	1.50	0.78	1.54	1.02
	20	0.97	1.45	0.47	0.83	1.33	0.50	1.43	1.07
	30	0.82	1.18	0.36	0.74	1.10	0.36	1.18	1.07
1000*50*200	20	0.94	1.54	0.59	0.80	1.46	0.66	1.53	1.04
	40	1.09	1.42	0.33	0.99	1.34	0.34	1.43	1.06
	60	0.99	1.19	0.21	0.92	1.13	0.21	1.22	1.07

Table 6: Fracture parameters of HSC1

Beam dimensions (mm)	Notch depth (mm)	Fracture parameters (MPa$\sqrt{}$m)						Crack extension resistance using Double – K model	
		Double-G model			Double-K model			$K_R(\Delta a_c) = K_{Ic}^{ini}(r) + K_{Ic}^{C}$	Ratio, $\frac{K_R(\Delta a_c)}{K_{Ic}^{un}}$
		K_{Ic}^{ini}	K_{Ic}^{un}	K_{Ic}^{C}	K_{Ic}^{ini}	K_{Ic}^{un}	K_{Ic}^{C}		
250*50*50	5	0.91	8.35	7.45	0.77	8.63	7.86	8.71	1.01
	10	0.92	7.75	6.83	0.97	8.10	7.13	7.96	0.98
	15	0.89	7.33	6.44	0.96	7.67	6.71	7.56	0.98
	20	0.89	6.68	5.79	0.93	6.98	6.05	6.92	0.99
500*50*100	10	1.00	8.95	7.94	0.84	9.11	8.27	9.23	1.01
	20	0.87	7.49	6.62	0.97	7.88	6.90	7.74	0.98
	30	0.86	6.89	6.03	0.76	7.06	6.30	7.16	1.01
	40	0.91	6.42	5.51	0.79	6.57	5.78	6.70	1.02

Table 7: Fracture parameters of UHSC

Beam dimensions (mm)	Notch depth (mm)	Fracture parameters (MPa$\sqrt{m}$)						Crack extension resistance using Double – K model	
		Double-G model			Double-K model			$K_R(\Delta a_c) = K_{Ic}^{ini}(r) + K_{Ic}^{C}$	Ratio, $\frac{K_R(\Delta a_c)}{K_{Ic}^{un}}$
		K_{Ic}^{ini}	K_{Ic}^{un}	K_{Ic}^{C}	K_{Ic}^{ini}	K_{Ic}^{un}	K_{Ic}^{C}		
250*50*50	5	2.27	13.87	11.59	1.74	13.85	12.11	14.15	1.02
	10	2.18	12.56	10.37	2.17	12.86	10.69	12.66	0.98
	15	2.18	11.50	9.31	2.35	11.96	9.61	11.68	0.98
	20	1.88	10.00	8.11	1.64	10.09	8.45	10.28	1.02
400*50*80	8	2.51	14.57	12.06	2.09	14.68	12.59	14.87	1.01
	16	2.26	12.91	10.64	2.29	13.28	10.99	13.12	0.99
	24	2.01	11.33	9.31	1.79	11.44	9.65	11.63	1.02
	32	1.92	10.17	8.24	1.89	10.50	8.61	10.52	1.01
650*50*130	13	2.35	15.27	12.91	1.90	15.34	13.44	15.54	1.01
	26	2.12	13.21	11.08	2.17	13.65	11.48	13.55	0.99
	39	2.02	11.94	9.919	1.84	12.13	10.29	12.33	1.02
	52	1.95	10.75	8.81	2.0	11.27	9.27	11.17	0.99

tained through double – K model. The computed fracture parameters will be useful for crack growth study, remaining life and residual strength evaluation of concrete structural components.

Acknowledgement: We acknowledge with thanks the valuable technical suggestions and support provided by our colleagues, Dr. G.S. Palani, Mr S. Maheshwaran, Ms. Smitha Gopinath, Mr V. Ramesh Kumar, Scientists and Ms. B. Bhuvaneswari, Quick Hire Fellow, during the course of this investigation. The help and support provided by the staff of Advanced Materials Laboratory, CSIR-SERC to carry out the experiments is greatly acknowledged. This paper is being published with the permission of the Director, CSIR- SERC, Chennai, India.

References

Bazant, Z.P.; Kim, J-K.; Pfeiffer, P.A. (1987): Determination of fracture energy from size effect and brittleness number. *ACI Mater J*; 84, pp.463–80.

Bazant, Z.P.; kim, J.K.; Pfeiffer, P.A. (1986): Nonlinear fracture properties from size effect tests. *Jl. Structural Engineering*, ASCE, 112(2), pp.289-307.

Bazant, Z.P.; Oh, B.H. (1983): Crack band theory for fracture of concrete. RILEM *Materials and Structures*, 16, pp. 155-177.

Cook, R.F.; Fairbanks, C.J. (1987): Mining strength characteristics. *Jl. Materials Research,* 3(3), pp.345-356.

Goltermann, P.; Johansen, V.; Palbol, L. (1997): Packing of Aggregates: An Alternate Tool to Determine the Optimal Aggregate Mix. *ACI Material Journal*, pp.435-443.

Hillerborg, A.; Modeer, M.; Petersson, P.E. (1976): Analysis of crack formation and crack growth in concrete by means of fracture mechanics and finite elements. *Cement and Concrete Research,* 6, pp.773–782.

Horii, H.; Ichinomiya, T. (1991): Observation of fracture process zone by laser speckle technique and governing mechanism in fracture of concrete. *Int J Fract.* 51, pp.19–29.

Hsueh, C.H.; Beacher, P.F. (1988): Evaluation of bridging stress from R-curve behaviour for nontransforming ceramics. *Jl. American ceramics Society*, 71(5), pp.234-237.

Irwin, G.R. (1958): Fracture. Handbuch der Physiik, Vol. VI, ed. Flugge, Springer, pp.551-590.

Jenq, Y.S.; Shah, S.P. (1985): Two parameter fracture model for concrete. *Journal of Engineering Mechanics*, 111(10), pp.1227–1241.

Jenq, Y.S.; Carpinteri, A. (1991): Fracture mechanics test methods for concrete. Report of Technical Committee 89-FMT fracture mechanics of concrete. test methods RILEM. Chapman Hall, London.

Karihaloo, B.L.; Nallathambi, P. (1990): Effective crack model for the determination of fracture toughness K_{Ic}^{s} of concrete. *Engng Fract Mech*; 35 (4–5), pp.637–45.

Kraft, J.M.; Sulivan, A.M.; Boyle, R.W. (1961): Effect of dimensions on fast fracture instability of notched sheets. In: Proceedings of the crack propagation symposium, Vol. I, College of Aeronatics, Cranfield, England, pp. 8-26.

Li, Y.N.; Liang R.Y. (1992): Stability theory of cohesive crack model. *Jl. Engg. Mechanics*, ASCE, 118(3), pp.587-603

Mingzhe, A. N.; Ziruo, Y. U.; Sun Meili; Zheng Shuaiquan; Liang Lei. (2010): Fatigue Properties of RPC under Cyclic Loads of Single-stage and Multi-level Amplitude. *Journal of Wuhan University of Technology-Material Science Ed.,* pp.167-173.

Rama Chandra Murthy, A.; Palani, G.S.; Nagesh R. Iyer; Smitha Gopinath. (2008): A methodology for remaining life prediction of concrete structural components accounting for tension softening effect. Computers and Concrete, 5(3), pp.261-277.

Reinhardt, H.W.; Xu, S. (1999): Crack extension resistance based on the cohesive force in concrete. *Engng. Fract. Mech.*, 64, pp.563-587.

Richard, P.; Cheyrezy, M. H. (1994): Reactive powder concretes with high ductility and 200–800 MPa compressive strength. *ACI SP144*, 24, pp.507–18.

Richard, P.; Cheyrezy, M. (1995): Composition of reactive powder concretes. *Cement and Concrete Research*, 25(7), pp.1501-1511.

Swartz, S.E.; Refai, T.M.E. (1987): Influence of size on opening mode fracture parameters for precracked concrete beams in bending. In: Shah SP, Swartz SE, editors. Proceedings of ESM-RILEM international conference on fracture of concrete and rock, Texas, Houston; pp.242–252.

Tada, H.; Paris, P.C.; Irwin, G.R. (1985): The Stress Analysis of Cracks Handbook. Paris Productions Incorporated, St. Louis, Missouri, USA.

Wecharatana, M.; Shah S.P. (1982): Slow crack growth in cement composites. *Jl. Structural Engineering, ASCE*, 108(6), pp.1400-1413.

Xu S.; Reinhardt, H.W. (1999): Determination of double-K criterion for crack propagation on quasi-brittle fracture. part I: experimental investigation of crack propagation. *Int J Fract*; 98(2), pp.111–49.

Xu, S.; Reinhardt, H.W. (2000): A simplified method for determining double-K

fracture parameters for three point bending tests. *Int. J. Fracture*, 104, pp.181-209.

Xu, S.; Reinhardt, H.W. (1999): Determination of double-K criterion for crack propagation on quasi-brittle fracture, part II: analytical evaluating and practical measuring methods for three-point bending notched beams. *Int J Fract;* 98 (2), pp.151–77.

Xu, S.; Reinhardt, H.W. (1998): Crack extension resistance and fracture properties of quasi-brittle softening materials like concrete based on the complete process of fracture. *Int J Fract*; 92(1), pp.71–99.

Zhao, Y.; Xu, S. (2002): An analytical study on the energy in fracture process of concrete. PhD thesis. Dalian University of Technology.

Xu, S.; Zhang, X. (2008): Determination of fracture parameters for crack propagation in concrete using an energy approach. *Eng. Fract. Mech.*, 75, pp.4292–4308.

Bazant, Z.P.; Kazemi, M.T. (1989): Size dependency of concrete fracture energy determined by RILEM work-of-fracture method. Report No 89-12/B623s, Northwestern University, Evanston.

RILEM Technical Committee 89-FMT. (1990): Determination of fracture parameters (K_{Ic}^{s} and CTODc) of plain concrete using tree-point bend tests, proposed RILEM draft recommendations. *Mater Struct*.; 23(138), pp.457–60.